



Contents lists available at ScienceDirect

## Arabian Journal of Chemistry

journal homepage: [www.ksu.edu.sa](http://www.ksu.edu.sa)Study of the effect of H<sub>2</sub>S on the diffusion and displacement of CH<sub>4</sub> in coalJinyu Li<sup>a,b,\*</sup>, He Ji<sup>a</sup>, Zunguo Zhang<sup>a,b</sup>, Gang Bai<sup>a,b</sup>, Hongbao Zhao<sup>c</sup>, Xihua Zhou<sup>a,b</sup>, Yueran Wang<sup>a</sup>, Yixin Li<sup>a</sup><sup>a</sup> College of Safety Science and Engineering, Liaoning Technical University, Huludao 125105, Liaoning, PR China<sup>b</sup> Key Laboratory of Mine Thermodynamic Disasters and Control of Ministry of Education (Liaoning Technical University), Huludao 125105, Liaoning, PR China<sup>c</sup> School of Energy and Mining Engineering, China University of Mining and Technology, Beijing 100083, PR China

## ARTICLE INFO

## Keywords:

Molecular simulation  
H<sub>2</sub>S  
CH<sub>4</sub> diffusion  
Displacement effects

## ABSTRACT

In order to address the issue of safe and efficient extraction of coalbed methane in H<sub>2</sub>S-containing coal mines, this study explored the impact of H<sub>2</sub>S on CH<sub>4</sub> diffusion and displacement within coal. The molecular structure model of Guizhou Linhua (LH) coal was obtained based on the structural physical characterization experiment of coal such as <sup>13</sup>C NMR, FTIR, XPS, we investigated the diffusion coefficient of CH<sub>4</sub> in coal under different fixed adsorption amounts of H<sub>2</sub>S and examined the corresponding adsorption curves of mixed gas (H<sub>2</sub>S, CH<sub>4</sub>, CO<sub>2</sub>) under varying component proportions using the molecular simulation software Materials Studio. The results indicate that when H<sub>2</sub>S is present in the adsorption system, lower levels of absorbed H<sub>2</sub>S content by coal correspond to higher CH<sub>4</sub> diffusion coefficients and improved diffusion effects. In other words, the presence of H<sub>2</sub>S inhibits CH<sub>4</sub> diffusion within coal. Under identical temperature and pressure conditions, the adsorption capacity of coal for CH<sub>4</sub>, H<sub>2</sub>S, and CO<sub>2</sub> follows this order: H<sub>2</sub>S > CO<sub>2</sub> > CH<sub>4</sub>. When the mixture  $n(\text{CO}_2)/n(\text{CH}_4)$  is in the range of 0–150 % and there is H<sub>2</sub>S influence in the system, there is a significant reduction in CH<sub>4</sub> adsorption capacity compared to two-component coals containing CO<sub>2</sub>/CH<sub>4</sub>, it becomes evident that H<sub>2</sub>S has an inhibitory effect on CO<sub>2</sub> displacing CH<sub>4</sub> within coal.

## 1. Introduction

With the gradual increase in the depth of coal resources mining, coal mine gas disasters occur frequently. According to valid statistics, China's coal and gas protruding mines a total of more than 600, gas explosion accidents present "more in the south and less in the north" geographic distribution of the trend, of which the number of accidents and the number of deaths in Guizhou, Sichuan and other places accounted for a relatively higher proportion, respectively, were 28.57 % and 28.85 % (Liang et al., 2023; Jing and Mu, 2023; Fan et al., 2023; Xu et al., 2023). As a common hazardous gas in underground coal mines, H<sub>2</sub>S poses a great threat to the safety of workers' lives and properties, and coal mine safety accidents caused by H<sub>2</sub>S have gradually become the main problem of coal mine safety production (Rubright et al., 2017; Tan et al., 2020; Yang et al., 2022; Zhang et al., 2020). Combined with the current situation of coal resources development in China, the development trend of coal and CBM co-mining has become mainstream (Zhang et al., 2022). The adsorption and diffusion property of CH<sub>4</sub> in coal matrix is an important reservoir parameter affecting the output of CBM, so analysing

and exploring the influencing factors of the diffusion property of CH<sub>4</sub> in coal is of great significance for the safe and efficient exploitation of coal and CBM resources in China.

Regarding the adsorption characteristics of CH<sub>4</sub>, in recent years, many scholars have concluded through macroscopic adsorption experiments or microscopic molecular simulation studies that there is a clear competition adsorption between H<sub>2</sub>S and CH<sub>4</sub>, and the adsorption capacity of H<sub>2</sub>S in coal is greater than that of CH<sub>4</sub> under the same conditions, and the presence of H<sub>2</sub>S is an important factor affecting the adsorption of CH<sub>4</sub> in coal body (He et al., 2016; Xue et al., 2017; Liu, 2020; Wang et al., 2020; Zhou, 2021). In terms of the diffusion characteristics of CH<sub>4</sub>, in 2016, Zhao et al. (Zhao et al., 2016) in order to deeply investigate the diffusion transport mechanism of CH<sub>4</sub> and CO<sub>2</sub> in CO<sub>2</sub>-ECBM project, used the technical means of molecular simulation to molecularly simulate the self-diffusion coefficients based on the Wiser coal model, and the study showed that the self-diffusion coefficient, the corrected diffusion coefficient and transport diffusion coefficients of CH<sub>4</sub> were smaller than those of CO<sub>2</sub>, and the study is expected to provide some theoretical guidance for the CO<sub>2</sub>-ECBM project. The study is

\* Corresponding author.

E-mail address: [18813131875@126.com](mailto:18813131875@126.com) (J. Li).<https://doi.org/10.1016/j.arabjc.2024.105779>

Received 6 March 2024; Accepted 3 April 2024

Available online 4 April 2024

1878-5352/© 2024 The Authors. Published by Elsevier B.V. on behalf of King Saud University. This is an open access article under the CC BY-NC-ND license (<http://creativecommons.org/licenses/by-nc-nd/4.0/>).

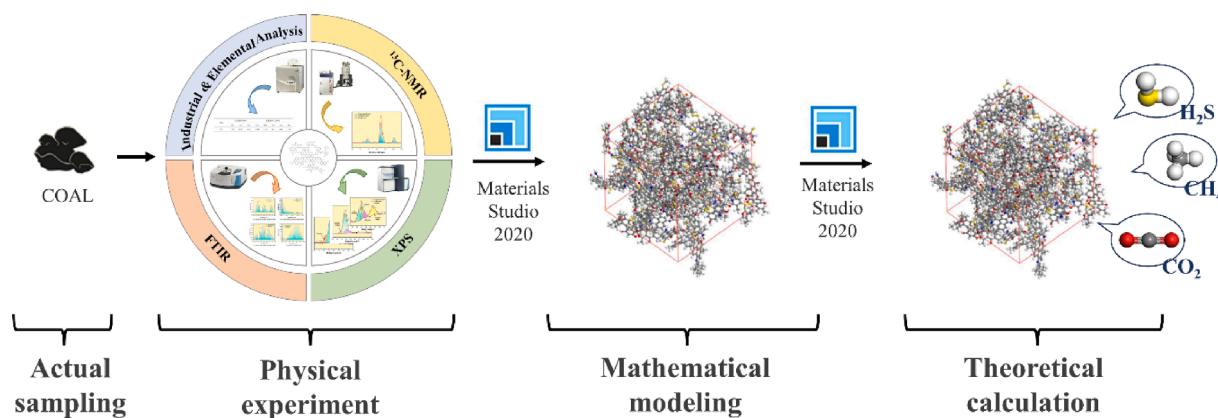


Fig. 1. Conceptual map of the research programme.

expected to provide some theoretical guiding data for the ECBM project; Meng et al. (Meng and Li, 2016) established the relationship and model between the diffusion coefficient of  $\text{CH}_4$  in coal and factors such as temperature and pressure through  $\text{CH}_4$  gas diffusion experiments, and analysed that the temperature, pressure, water content and the degree of coal metamorphism are the factors affecting the diffusion of  $\text{CH}_4$  in coal, and the study revealed the diffusion mechanism of  $\text{CH}_4$  in coal, which is of great theoretical and practical significance for the development of coalbed methane; Zhao et al. (Zhao et al., 2016) tested the diffusion coefficients of coal matrix by testing the diffusion coefficients of coal samples with different degrees of metamorphism, and concluded that the diffusion coefficients of coal decreased firstly and then increased with the increase of the degree of metamorphism of coal. In 2019, Meng et al. (Meng et al., 2019) calculated the diffusion coefficient of  $\text{CH}_4$  gas in coal by applying the unitary pore structure gas unsteady diffusion model through  $\text{CH}_4$  isothermal adsorption experiments in order to reveal the diffusion law and control mechanism of  $\text{CH}_4$  in coal, and the study concluded that the diffusion coefficient of  $\text{CH}_4$  in coal increased with the increase of pressure, and that the effective diffusion coefficient and diffusion coefficient of the dry coal samples were larger than those of the equilibrium moisture samples under the condition of the same temperature and same pressure. In 2021, Tang et al. (Tang et al., 2021) used a molecular dynamics simulation method to investigate the effects of pressure, temperature,  $\text{CO}_2$  and  $\text{H}_2\text{O}$  on the diffusion of  $\text{CH}_4$  in coal, which showed that the diffusion coefficients of  $\text{CH}_4$  molecules decreased with the increase of the volume fraction of  $\text{CO}_2$ , and the inhibition of the diffusion of  $\text{CH}_4$  molecules in the coal seams was stronger with the increase of the volume fraction of  $\text{CO}_2$  compared with that of  $\text{H}_2\text{O}$ , which indicated that the coal seam injection of  $\text{CO}_2$  extraction method was more effective in terms of the molecular dynamics of the diffusion coefficients. In 2022, Jing et al. (Jiang et al., 2022) investigated the influence of moisture on the diffusion characteristics of  $\text{CH}_4$  in low-rank coals, and carried out  $\text{CH}_4$  desorption experiments under different water content conditions, which showed that moisture significantly reduced the diffusion capacity of low-rank coals, and that the competitive adsorption between moisture and  $\text{CH}_4$  molecules was an important factor influencing the diffusion characteristics of  $\text{CH}_4$  in coals. Sun et al. (Sun et al., 2022) in order to explore the competitive adsorption law of  $\text{CO}_2/\text{N}_2$  in coal seams, they used molecular simulation software to establish coal molecular model and based on the Giant Canonical Monte Carlo (GCMC) method, they investigated the influence of each stage on  $\text{CH}_4$  adsorption in  $\text{CO}_2/\text{N}_2$  alternating coalbed methane technology, and the results showed that  $\text{CH}_4$  was rapidly desorbed from coal in the injection stage of  $\text{CO}_2$ , and the adsorption amount of  $\text{CH}_4$  and  $\text{CO}_2$  was reduced after transferring to  $\text{N}_2$  injection, when  $\omega(\text{N}_2)/\omega(\text{CO}_2) = 0.6$  or so, the desorption amount of  $\text{CH}_4$  is the maximum value, which is most favourable to the development of coalbed methane, and the research concept is of great significance for exploring the influencing factors of

**Table 1**  
Industrial and elemental analysis of coal samples.

| Sample | Industrial analysis/% |                 |                  | Elemental analysis/% |                  |                  |                  |                  |
|--------|-----------------------|-----------------|------------------|----------------------|------------------|------------------|------------------|------------------|
|        | $M_{\text{ad}}$       | $A_{\text{ad}}$ | $V_{\text{daf}}$ | $C_{\text{daf}}$     | $H_{\text{daf}}$ | $O_{\text{daf}}$ | $N_{\text{daf}}$ | $S_{\text{daf}}$ |
| LH     | 2.09                  | 15.67           | 8.54             | 85.68                | 5.29             | 4.85             | 0.94             | 3.24             |

Note: The C, H, N, S elements are the average of two parallel tests, and the O elements are obtained by difference subtraction.

the process of  $\text{CH}_4$  displacement by  $\text{CO}_2$ .

In summary, in the research of  $\text{CH}_4$  diffusion characteristics and  $\text{CO}_2$  driving  $\text{CH}_4$  influencing factors in coal, many scholars at home and abroad have carried out more systematic research and achieved rich results, but the research on the effect of  $\text{H}_2\text{S}$  on the two needs to be further improved. So on this basis, the use of a combination of experimental and simulation methods, the analysis of the construction of a complex coal macromolecular structure model, based on molecular mechanics and molecular dynamics, to understand the effect of  $\text{H}_2\text{S}$  on the  $\text{CH}_4$  diffusion characteristics in coal. Based on molecular mechanics and molecular dynamics, we analyse the effect of  $\text{H}_2\text{S}$  on the diffusion characteristics of  $\text{CH}_4$  in coal from a microscopic point of view, and analyse the effect of  $\text{H}_2\text{S}$  in the process of  $\text{CO}_2$  driving  $\text{CH}_4$ , as shown in Fig. 1. Which will help us to understand the diffusion and transport mechanism of  $\text{CH}_4$  in coal, and at the same time, it has a theoretical guiding significance for the safe mining of coal and the highly efficient coalbed methane extraction in the coal mine containing  $\text{H}_2\text{S}$ .

## 2. Construction of coal macromolecular model

### 2.1. Preparation of coal sample

In this paper, the research coal samples were taken from Linhua coal samples (LH) of a mine in Linhua, Guizhou, crushed by a coal mill and sieved to 200 mesh, and then dried to constant weight in a drying box at  $40\text{ }^\circ\text{C}$  to dry the excess moisture on the surface of the coal samples, and then quickly loaded into a sealed bag for storage, and then characterized the structure of the coal macromolecular compounds and constructed a complex coal macromolecular structure model by carrying out physical testing experiments such as industrial and elemental analyses of the coal samples. According to the national standard ‘‘Industrial Analysis Methods of Coal’’ (GB/T212-2008) and the national standard regulations (GB/T476-2008), the coal samples were subjected to industrial and elemental analyses respectively, and the results of the analyses are shown in Table 1:

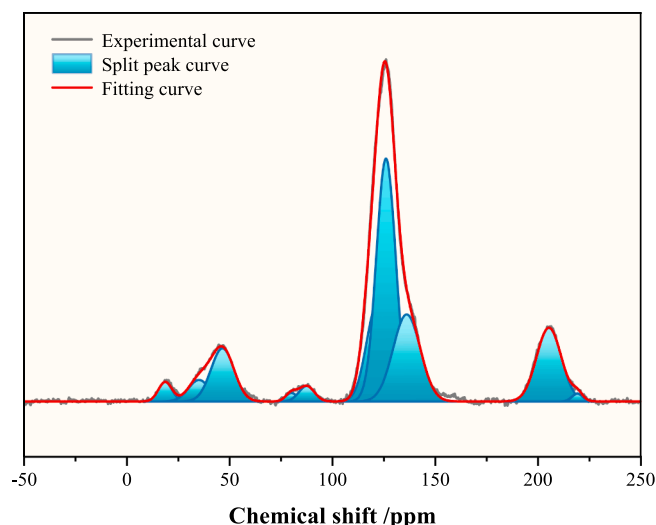


Fig. 2. Split-peak spectrum of LH solid NMR carbon spectrum.

## 2.2. Coal molecular structure characterization

### 2.2.1. $^{13}\text{C}$ nuclear magnetic resonance ( $^{13}\text{C}$ NMR)

The  $^{13}\text{C}$  NMR technique is a physical method to directly obtain the information on the distribution of carbon and hydrogen atoms in coal samples and the ratio of bridged carbon to *peri*-carbon. Experimentally, 0.3 g of coal samples were taken through BRUKER AVANCE NEO 400WB equipment, tested without internal standard, the reference material is TMS (0 ppm), and the solid-state NMR carbon spectra of the coal samples were analyzed and determined by CP MAS NMR (cross-polarization magic angle rotational NMR) test method. The original spectra were processed by peak fitting in the range of  $-50$  ppm  $\sim$   $250$  ppm using Origin software (Fig. 2).

When exploring the chemical structure of coal macromolecules, the aromatic bridged carbon and *peri*-carbon ratio of coal samples ( $X_{\text{BP}}$ ) is an important characterisation parameter for the degree of condensation of aromatic compounds in the molecular structure of coal (Eq. (1)).

$$X_{\text{BP}} = f_a^{\text{B}} / (f_a^{\text{H}} + f_a^{\text{P}} + f_a^{\text{S}}) \quad (1)$$

where  $X_{\text{BP}}$  is the Bridge carbon to carbon ratio,  $f_a^{\text{B}}$  is the aromatic bridgehead C,  $f_a^{\text{H}}$  is the protonated and aromatic,  $f_a^{\text{P}}$  is the aromatic C bonded hydroxyl or ether oxygen,  $f_a^{\text{S}}$  is the alkylated aromatic.

Combined with the peak position and area percentage of each sub-peak obtained by fitting, the relevant structural parameters of the coal samples were calculated based on the attribution of the functional groups and the corresponding chemical shifts by  $^{13}\text{C}$  NMR, and the results are shown in Table 2. Calculated from Eq. (1), the  $X_{\text{BP}}$  of the LH coal sample is 0.33, and this parameter can be used to calculate the aromatic size and aromatic type.

### 2.2.2. Fourier infrared spectroscopy (FTIR)

The infrared spectra obtained by the FTIR technique can reflect the information of the chemical structure of the substance, such as the fat carbon content and oxygen-containing functional groups. In the experiment, 10 mg of coal samples were taken, and the samples were

**Table 2**  
Structural parameters of LH coal.

| Sample | $f_a$ | $f_a^{\text{C}}$ | $f_a^{\text{A}}$ | $f_a^{\text{N}}$ | $f_a^{\text{H}}$ | $f_a^{\text{P}}$ | $f_a^{\text{S}}$ | $f_a^{\text{B}}$ | $f_{\text{al}}$ | $f_{\text{al}}^*$ | $f_{\text{al}}^{\text{H}}$ | $f_{\text{al}}^{\text{O}}$ |
|--------|-------|------------------|------------------|------------------|------------------|------------------|------------------|------------------|-----------------|-------------------|----------------------------|----------------------------|
| LH     | 82.65 | 13.15            | 69.50            | 20.26            | 49.24            | 0.00             | 3.01             | 17.25            | 17.35           | 2.15              | 10.15                      | 5.05                       |

Note:  $f_a$ - total aromatic carbon,  $f_a^{\text{C}}$ - carbonyl or carboxyl group,  $f_a^{\text{A}}$ - aromatic C,  $f_a^{\text{N}}$ - nonprotonated and aromatic,  $f_a^{\text{H}}$ - protonated and aromatic,  $f_a^{\text{P}}$ - aromatic C bonded hydroxyl or ether oxygen,  $f_a^{\text{S}}$ - alkylated aromatic,  $f_a^{\text{B}}$ - aromatic bridgehead C,  $f_{\text{al}}$ - total sp<sup>3</sup> hybridized,  $f_{\text{al}}^*$ - CH<sub>3</sub> or nonprotonated,  $f_{\text{al}}^{\text{H}}$ - CH or CH<sub>2</sub>,  $f_{\text{al}}^{\text{O}}$ - aliphatic C bonded oxygen.

thoroughly ground with dry KBr powder and then placed on a tablet press. The infrared spectra of the samples were collected by a Thermo Scientific Nicolet iS20 device in the United States of America, with a resolution of  $4\text{ cm}^{-1}$ , and a number of scans of 32, with a range of wave numbers of  $400\text{--}4000\text{ cm}^{-1}$ .

Four regions of the infrared spectral map: aromatic hydrocarbon absorption band ( $700 \sim 900\text{ cm}^{-1}$ ), oxygen-containing functional groups and part of the aliphatic hydrocarbon absorption band ( $1000 \sim 1800\text{ cm}^{-1}$ ), aliphatic hydrocarbon absorption band ( $2800 \sim 3000\text{ cm}^{-1}$ ), and hydroxyl absorption band ( $3000 \sim 3600\text{ cm}^{-1}$ ) were peak-fitted by using Origin software (Fig. 3).

After split peak fitting, the split peak results of the infrared spectra were attributed to each sub-peak, which was thus obtained:

(1) From the fitting of the infrared spectra of the aromatic structure of LH coal samples, it can be obtained that there are three main peaks in the figure, among which  $740\text{ cm}^{-1}$  is attributed to the benzene ring disubstitution,  $800\text{ cm}^{-1}$  is attributed to the benzene ring trisubstitution, tetrasubstitution,  $860\text{ cm}^{-1}$  is attributed to the benzene ring quintuple substitution; the analysis of the relative areas of the nine subpeaks in the region after attribution respectively shows that, in the aromatic structure of LH coal samples, all types of benzene ring substitutions and their percentages are: benzene ring disubstitution (42.06 %), benzene ring trisubstitution (32.85 %), benzene ring tetrasubstitution (12.12 %), benzene ring pentasubstitution (12.97 %).

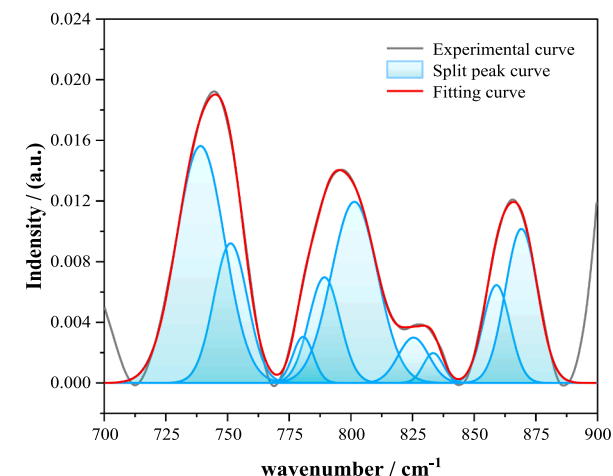
(2) The fitting of the infrared spectra of the oxygenated functional groups of LH coal samples shows that the characteristic peaks within the range of  $1000\text{ cm}^{-1}$  to  $1050\text{ cm}^{-1}$  are attributed to the ash in the coal, which is caused by the fact that no deashing was carried out for the coal samples before the infrared analysis; the relative areas of the 13 sub-peaks in the region are analysed after attributing them to each sub-peak to obtain the relative areas of each sub-peak. The main presence of oxygen-containing functional groups in the molecular structure in the form of phenols, alcohols, ethers, esters of C-O ( $1110\text{--}1330\text{ cm}^{-1}$ ) accounted for 40.7 %, while the presence of a smaller proportion of carbonyl.

(3) From the fitting of the infrared spectra of aliphatic hydrocarbons of LH coal samples, it can be obtained that there are three main peaks in the vicinity of the wave numbers of  $2830\text{ cm}^{-1}$ ,  $2890\text{ cm}^{-1}$  and  $2940\text{ cm}^{-1}$ , respectively. After the 9 sub-peaks in this region are classified and combined with the relative areas of each sub-peak, the relative areas of symmetrical and asymmetric CH<sub>x</sub> stretching vibration peaks in the molecular structure of LH coal samples are 30.42 % and 31.95 %, respectively. The relative area of CH<sub>3</sub> is larger than that of CH<sub>2</sub>, and the ratio of the two peaks is 2.94, indicating that the carbon chains in the molecular structure of LH coal samples are mainly short and medium chains, and there are more side chains.

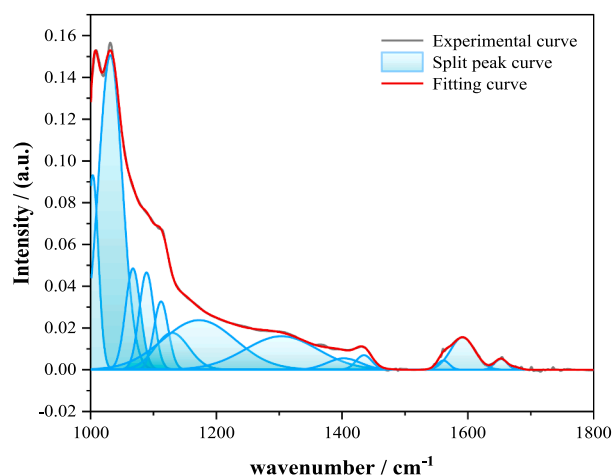
(4) The infrared spectra of the hydrocarbon structure of the LH coal samples showed that there was a main peak in the vicinity of the wave number of  $3400\text{ cm}^{-1}$ , and the 5 sub-peaks in the region were attributed to the relative areas of the peaks, which showed that the main forms of hydroxyl structure in the molecular structure of the LH coal samples and their proportions were the self-consolidated hydroxyl bonding (66.12 %), hydroxyl cyclic polymers (26.81 %), and the cyclic structure of the hydroxyl bonding (7.07 %).

### 2.2.3. X-ray photoelectron spectroscopy (XPS)

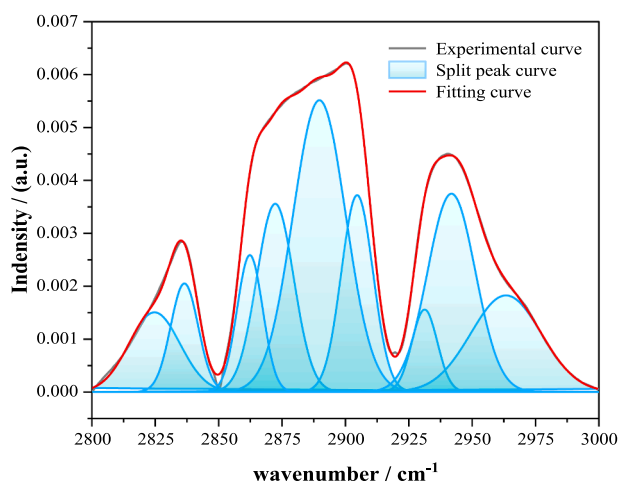
The XPS technique is based on the Einstein photoelectron dispersion



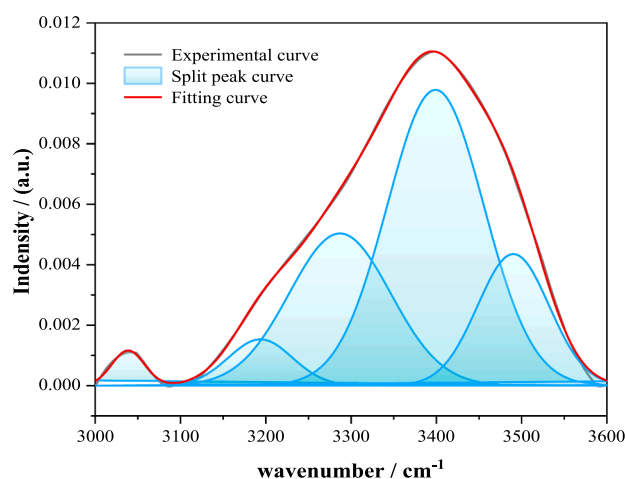
(a) aromatic hydrocarbon absorption band



(b) oxygen-containing functional groups band



(c) aliphatic hydrocarbon absorption band



(d) hydroxyl absorption band

Fig. 3. Fitting of infrared spectra of LH coal samples in the range of 700–3600  $\text{cm}^{-1}$ .

formula, which can be used to image the elements and their chemical valences, and give the distribution images of different chemical states of different elements on the surface. After taking 30 mg of coal samples, we analysed the C, O, N and S elements in coal by Thermo Scientific K-Alpha equipment, in which the full-spectrum scanning fluence energy was 150 eV with a step size of 1 eV, and the narrow-spectrum scanning fluence energy was 50 eV with a step size of 0.1 eV. We obtained the spectra of  $\text{N}_{1s}$ ,  $\text{O}_{1s}$ , and  $\text{S}_{2p}$  by the experiment, and fitted the peaks to the spectra by using the Origin software (Fig. 4).

Combined with the peak fitting results of the spectra of each element and the XPS electron binding energy comparison table, the analyses can be specific to the assignment patterns of O, N and S elements in LH coal:

(1) In the LH coal  $\text{N}_{1s}$  spectrum, the relative area of the characteristic peak of pyrrole-type nitrogen (N-5) located at 400.42 eV is 70.35 %, the characteristic peak of pyridine-type nitrogen (N-6) near 398.46 eV is 13.77 %, and the quaternary nitrogen (N-Q) located at 401.95 eV and nitrogen oxides (N-X) located at 403.22 eV are 7.80 %, respectively, 8.08 %.

(2) In the LH coal  $\text{O}_{1s}$  spectrum, the relative area of the carbonyl (C = O) peak located at 531.61 eV is 73.34 %, the ether oxygen (C-O) located at 532.59 eV is 18.44 %, and the fitted peaks located at 530.21 and 536.08 eV belong to the inorganic and adsorbed oxygen peaks,

which are 6.68 % and 1.54 %, respectively.

(3) In the LH coal  $\text{S}_{2p}$  spectrum, the attribution of the characteristic peaks and their percentages are as follows: 162.86 eV (iron disulfide) characteristic peaks accounted for 24.75 %, 164.07 eV (thiophene) characteristic peaks accounted for 21.95 %, 165.25 eV (sulphoxide) characteristic peaks accounted for 15.02 %, and 169.164 eV (sulphone sulphur) characteristic peaks accounted for 38.28 %.

### 2.3. Construction of complex coal macromolecular model

From the above, it can be seen that the  $X_{BP}$  of LH coal is 0.33, and since the  $X_{BP}$  of benzene ring is 0, the  $X_{BP}$  of naphthalene ring is 0.25, and the  $X_{BP}$  of phenanthrene and anthracene is 0.4, the molecular structure of LH coal is mainly dominated by the 2 and 3 rings, and supplemented by the 1, 4 and 5 rings. In order to make its  $X_{BP}$  value close to the experimental calculation value, the number of each aromatic structure type in the coal molecular configuration was adjusted by the method of coefficient to be determined, and the results are shown in Table 3, at this time, the  $X_{BP}$  value was 0.325, and the total number of aromatic carbons was 175.

From the results of industrial and elemental analyses, it's known that LH coal belongs to the typical coal and the carbon mass fraction is 87.14

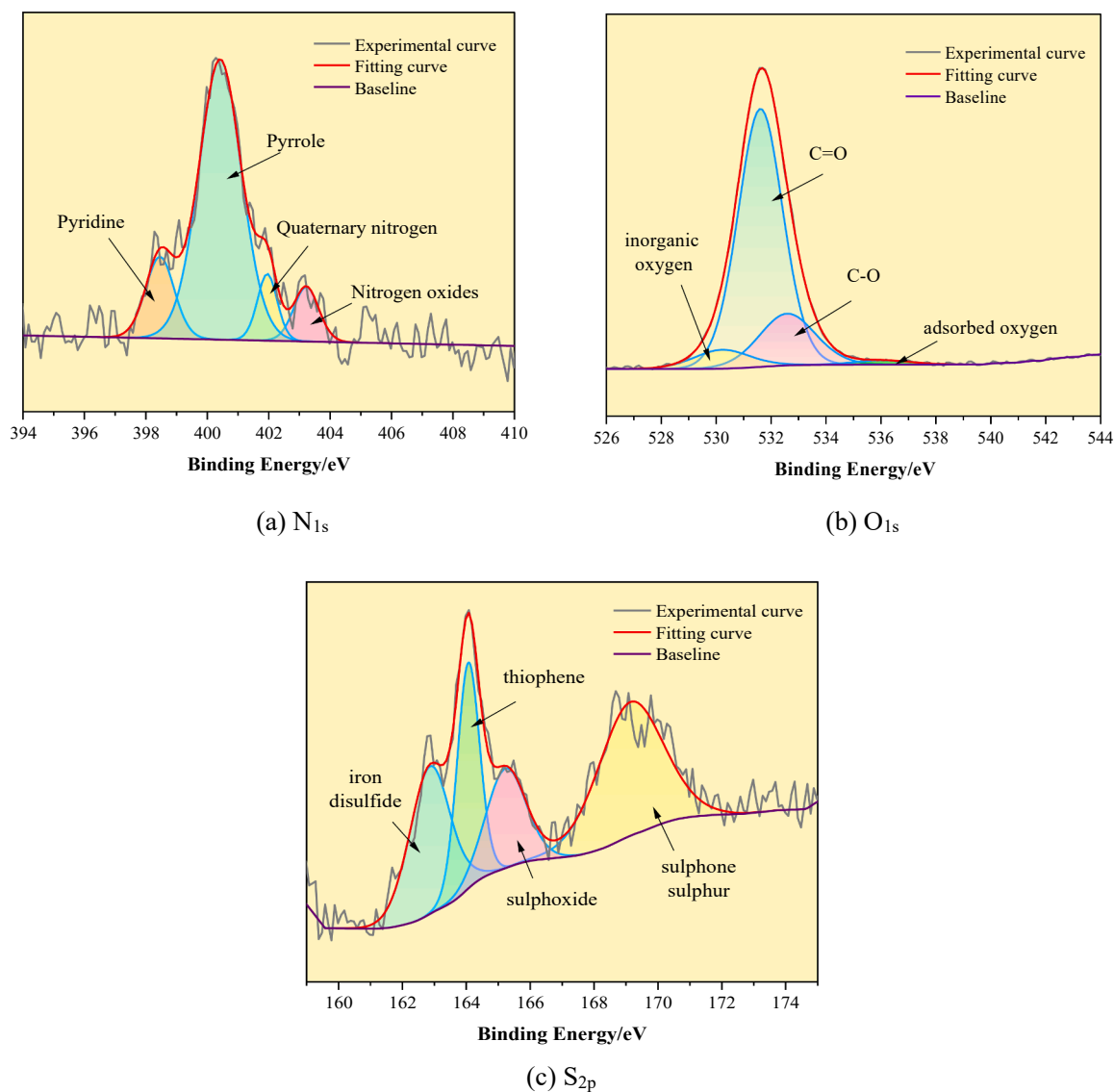


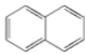
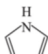
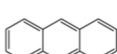
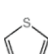
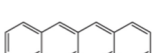
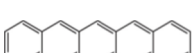


Fig. 4. XPS fitted spectra of N, O and S elements of LH coal.

**Table 3**  
Aromatic structures in the structure of LH coal.

| Type  | Number | Type  | Number |
|---|--------|---|--------|
|  | 1      |  | 1      |
|  | 6      |  | 1      |
|  | 4      |  | 1      |
|  | 1      |  | 1      |

%, so its molecular structure is dominated by the short-chain alkyl side chains, and according to the results of  $^{13}C$  NMR, it is known that the aromatic carbon rate of LH coal is 82.65 %, and the aliphatic carbon accounts for 17.35 %, and the preliminary calculation of the total number of carbon atoms of the LH coal is 212, and the number of aliphatic carbons is 37. Combined with the results of the previous

analysis, all kinds of atoms were added in turn to improve the coal macromolecular structure, and the LH coal macromolecular structure was drawn using ChemDraw drawing software, and the chemical shifts of the carbon atoms were calculated using this software, and the coal model was adjusted and corrected to make the  $^{13}C$  NMR spectrum calculated by the software similar to that obtained by the experiment, and the final macromolecular planar structural model of the LH coal was shown in Fig. 5, and its molecular formula is  $C_{212}H_{156}O_9N_2S_3$ .

The planar model of LH coal molecule was imported into MS molecular simulation software for hydrogen saturation. Based on the COMPASS II force field, the geometry optimisation and annealing kinetic optimisation of the coal molecule were carried out by using the Forcite module to obtain the three-dimensional structural model of coal macromolecule, which is the global energy minimum structure. A periodic structure equipped with 10 LH coal macromolecules was constructed using the AC module, and the kinetic relaxation at 298.15 K and NPT system was repeated after the optimisation of this periodic structure, with a total simulation time step of 500 ps, to obtain the standard LH coal macromolecule structural model (Fig. 6).

The cell equilibrium density of the LH complex coal macromolecule model obtained by molecular dynamics is  $1.38 \text{ g/cm}^3$ , which is slightly lower than the true density of the LH coal samples of  $1.41 \text{ g/cm}^3$ . This is

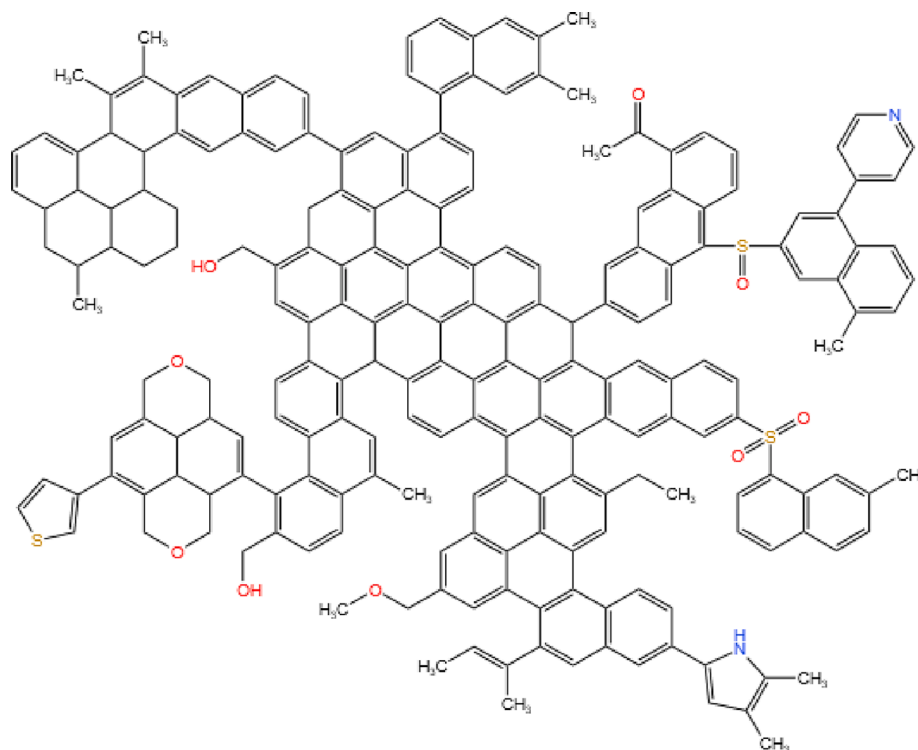


Fig. 5. Planar molecular structure of LH coal.

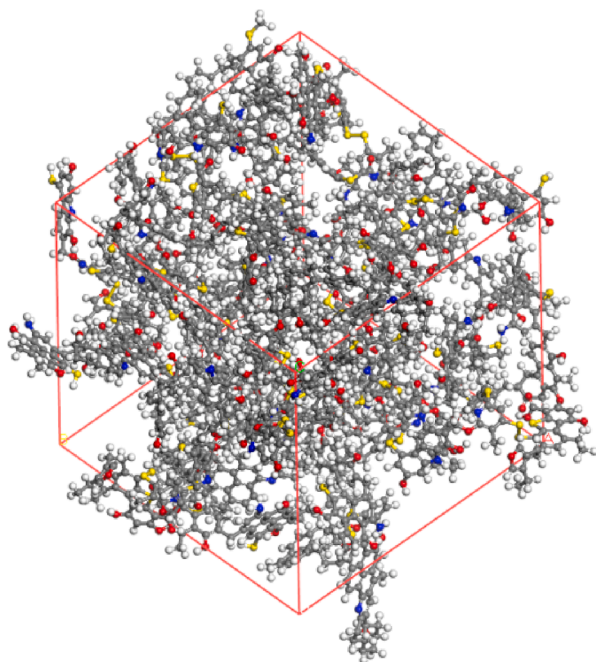


Fig. 6. Model of LH coal macromolecular structure.

mainly due to the fact that there are part of minerals in the actual coal samples, and the model construction process only takes into account the corresponding organic components in the coal, so there is a possibility that the modelled density is slightly less than the density of the actual coal. For this reason, the model density of LH coal macromolecular structure is reasonable.

#### 2.4. Calculation principle and method

In order to investigate the influence of H<sub>2</sub>S on the diffusion characteristics of CH<sub>4</sub> in coal, based on the above complex coal macromolecules, we constructed the structural model of CH<sub>4</sub> saturated adsorbed coal macromolecule with different content of H<sub>2</sub>S. Using the Sorption-Locate task, the number of molecules of the adsorbent H<sub>2</sub>S was fixed to 0, 5, 10, 15, respectively, and the adsorbed number of CH<sub>4</sub> was gradually increased. By comparing the trend of the total energy of the system, the corresponding CH<sub>4</sub> saturated adsorption number was determined, and the model of CH<sub>4</sub> saturated adsorption of coal macromolecules with the number of H<sub>2</sub>S fixed was obtained.

Based on the principle of molecular dynamics (MD), the saturated adsorption conformation of CH<sub>4</sub> is taken as the object of study, and its molecular dynamics is optimised under the NVT and NPT synthesis, and the mean-square displacement curves of CH<sub>4</sub> in coal molecules with different numbers of H<sub>2</sub>S are calculated analytically, so as to characterize the diffusion properties of CH<sub>4</sub> in coal under different systems by diffusion coefficients.

The diffusion coefficient can be calculated from can be calculated from Einstein's law of diffusion:

$$D_{\text{self}} = \lim_{t \rightarrow \infty} \frac{1}{6t} \left[ \frac{1}{N_t} \sum_{i=1}^N |r_i(t) - r_i(0)|^2 \right] \quad (2)$$

where:  $D_{\text{self}}$  is CH<sub>4</sub> self-diffusion coefficient, m<sup>2</sup>/s.  $N$  is the total number of CH<sub>4</sub> molecules.  $N_t$  is the average number of molecular dynamics steps, steps.  $t$  is the simulation time, ps.  $r_i(0)$  is the displacement of the center of mass of the  $i$ -th particle at the initial time, nm.  $r_i(t)$  is the displacement of the center of mass of the  $i$ -th particle at time  $t$ , nm.

Based on the mean-square displacement formula of the system can be obtained:

$$k_{\text{MSD}} = \lim_{t \rightarrow \infty} \frac{1}{6t} \left[ \frac{1}{N_t} \sum_{i=1}^N |r_i(t) - r_i(0)|^2 \right] \quad (3)$$

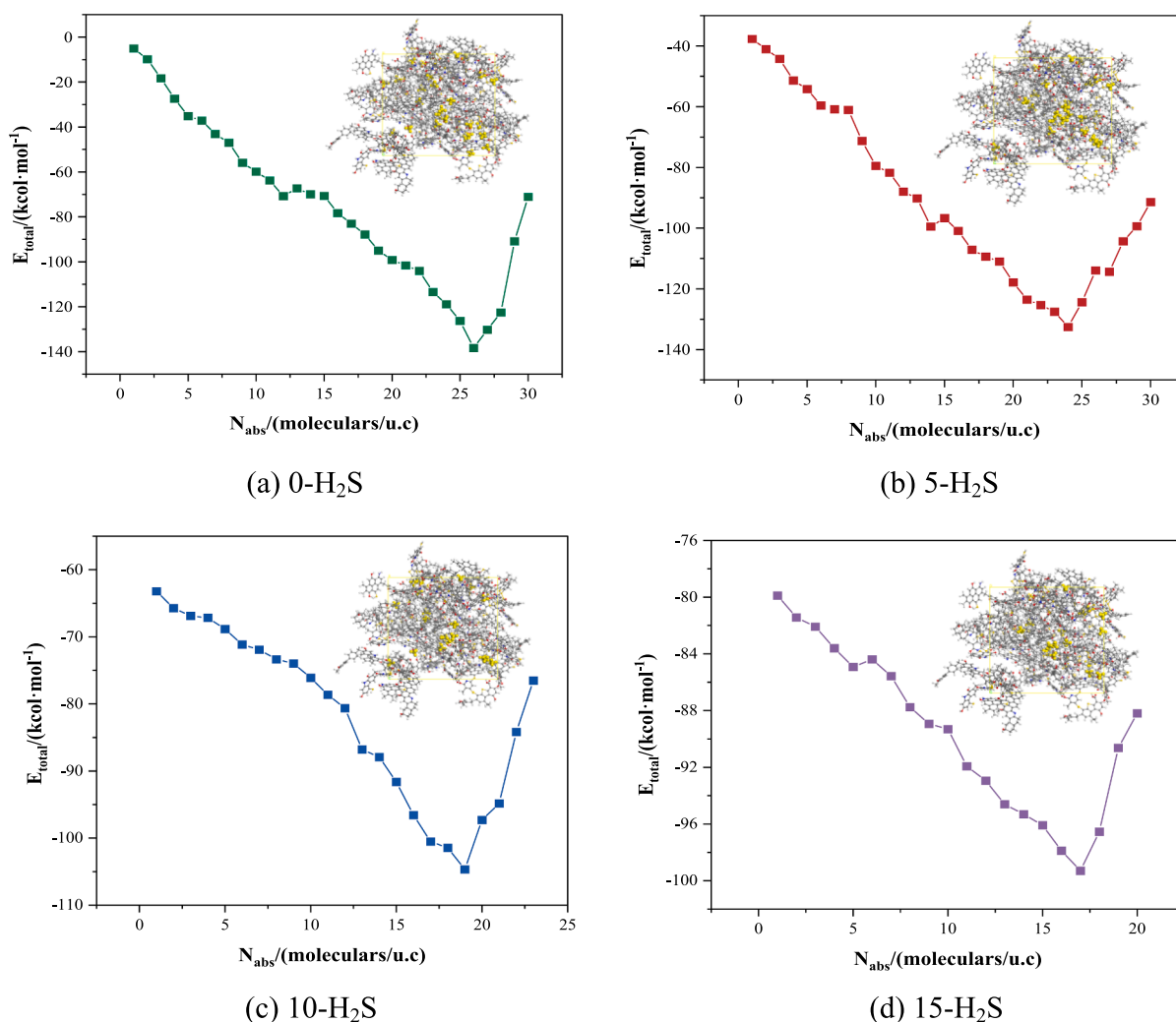


Fig. 7. Trend of  $E_{\text{total}}$  corresponding to different numbers of  $\text{H}_2\text{S}$  and  $\text{CH}_4$  molecules adsorbed.

$$D_{\text{self}} = \frac{1}{6} k_{\text{MSD}} \quad (4)$$

This gives 1/6 of the slope of the straight line after fitting a linear regression to the MSD curve as the diffusion coefficient.

The saturated adsorption amount of  $\text{CH}_4$  obtained by Sorption module refers to the number of  $\text{CH}_4$  adsorbed in a single crystal cell, whose unit is molecules/(u.c), and the actual common unit is mmol/g, and the principle of conversion between the two is shown in Eq. (5):

$$1 \text{ molecules}/(\text{u.c}) = \frac{10^3}{(N \times M)} \text{ mmol/g} \quad (5)$$

where:  $N$  is Avogadro's constant ( $6.02 \times 10^{23}$ ),  $M$  is the cell unit mass, g.

In the analysis and study of the effect of  $\text{H}_2\text{S}$  on  $\text{CO}_2$  to displace  $\text{CH}_4$ , the molar amount of  $\text{CH}_4$  in the ternary mixture was set as the saturated adsorption amount of coal macromolecules on  $\text{CH}_4$ , the molar amount of  $\text{H}_2\text{S}$  was set as 0, 1/3, 2/3, 3/3 of the molar amount of  $\text{CH}_4$ , and the molar amount of  $\text{CO}_2$  was set as 0%~150% of the molar amount of  $\text{CH}_4$  (every 10% was evenly divided into 15 groups) to achieve the control of the amounts of  $\text{CH}_4$ ,  $\text{H}_2\text{S}$  and  $\text{CO}_2$  in the mixture. According to the corresponding fugacity values of each component of the ternary gas, the adsorption simulation of coal macromolecules on different ratios of the ternary mixture under the condition of constant temperature and pressure was realized by using the Fixed Pressure task, and the trend of the saturated adsorption number of each adsorbent was obtained under the condition of different ratios of the mixture, so as to analyse the effect of

$\text{H}_2\text{S}$  on the displacement of  $\text{CH}_4$  by  $\text{CO}_2$  in the coal.

### 3. Effect of $\text{H}_2\text{S}$ on $\text{CH}_4$ diffusion in coal

#### 3.1. Simulation of $\text{CH}_4$ saturation adsorption of coal molecules

Before exploring the effect of  $\text{H}_2\text{S}$  on the diffusion of  $\text{CH}_4$  in coal, the number of saturated adsorbed  $\text{CH}_4$  corresponding to coal macromolecules with fixed  $\text{H}_2\text{S}$  adsorption number should be calculated, which provides a basic model for analysing and calculating the diffusion coefficient of  $\text{CH}_4$  under different  $\text{H}_2\text{S}$  content conditions.

$\text{H}_2\text{S}$  and  $\text{CH}_4$  molecules were used as adsorbents, where  $\text{H}_2\text{S}$  molecules were fixed at 0, 5, 10 and 15, and  $\text{CH}_4$  molecules were increased one by one, and multiple adsorption simulations were carried out sequentially by using the Sorption-locate task, and the simulation calculations yielded the trend of the total energy ( $E_{\text{total}}$ ) change for each system as shown in Fig. 7.

When the number of  $\text{CH}_4$  molecules adsorbed in the system reached saturation, all the surface active sites on the coal macromolecule had been occupied by adsorbates, and when the number of  $\text{CH}_4$  molecules exceeded the number of saturated adsorption, the repulsion between the coal macromolecule and  $\text{CH}_4$  molecules would be generated, which resulted in the upward trend of the total energy of the system. As shown in the figure above, with the gradual increase of the number of  $\text{CH}_4$  molecules adsorbed by the coal body, the total energy of the adsorption system of the four groups showed a trend of decreasing and then

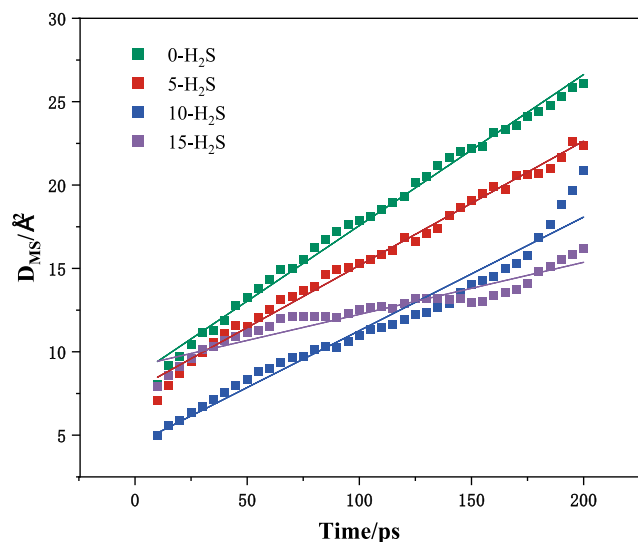


Fig. 8. MSD curves of CH<sub>4</sub> in coal bodies with different numbers of H<sub>2</sub>S adsorption.

Table 4

Diffusion coefficients of CH<sub>4</sub> in coal bodies with different H<sub>2</sub>S adsorption numbers.

| Fixed H <sub>2</sub> S number | Equation of linear regression | Diffusion coefficient/<br>(10 <sup>-9</sup> m <sup>2</sup> ·s <sup>-1</sup> ) |
|-------------------------------|-------------------------------|---|
| 0                             | $y = 0.0906x + 8.508$         | 0.151   |
| 5                             | $y = 0.0745x + 7.724$         | 0.124   |
| 10                            | $y = 0.0681x + 4.451$         | 0.114   |
| 15                            | $y = 0.0312x + 9.121$         | 0.052   |

increasing, when the coal macromolecule fixed adsorption of 0, 5, 10, 15 H<sub>2</sub>S molecules, the number of saturated adsorption of CH<sub>4</sub> corresponds to 26, 24, 19, 17, so the CH<sub>4</sub> saturated adsorption model of coal macromolecules under different H<sub>2</sub>S content can be obtained. Analysing the CH<sub>4</sub> adsorption process of coal macromolecules with different H<sub>2</sub>S adsorption numbers, it can be obtained that the presence of H<sub>2</sub>S in the system will preferentially seize the adsorption sites of the coal body, inhibit the adsorption of CH<sub>4</sub> molecules by the coal body.

### 3.2. CH<sub>4</sub> diffusion characteristics at different H<sub>2</sub>S contents

The saturated adsorption configuration of coal macromolecule CH<sub>4</sub> with different H<sub>2</sub>S adsorption numbers was taken as the initial model, and the geometry optimization and molecular dynamics simulation were carried out on the initial model by using the MS-Forcite module. Since the cell was constructed with a reasonable density when constructing the cell, there was no need to select the NPT system to further optimize the density when relaxing the cell, and the NVT system was selected to carry out the molecular dynamics calculation, and the kinetic simulation under the NVE system was continued on the completed configuration. After the calculation of the configuration, the kinetic simulation under the NVE system was continued, and the final trajectory file containing the equilibrium configuration was analysed to obtain the mean-square displacement curve of CH<sub>4</sub> in the coal macromolecule, and the results of the calculation are shown in Fig. 8. From the figure, it is obvious that the mean square displacement of CH<sub>4</sub> in each adsorption system is linearly related to the simulation time, so a linear regression was carried out on the four sets of MSD curves, and the diffusion coefficients of CH<sub>4</sub> in coal macromolecules with different number of H<sub>2</sub>S adsorption can be obtained according to the calculation of Eq. (4), and the results are shown in Table 4.

As can be obtained from the table, under the condition of 298.15 K

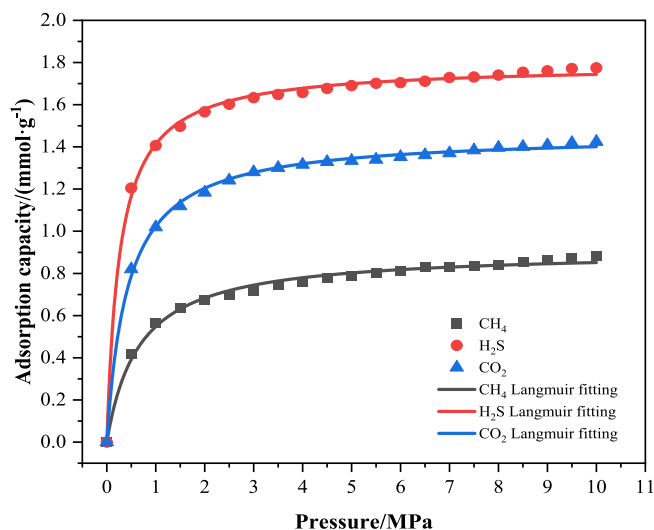


Fig. 9. Isothermal adsorption curves of each adsorbent in LH coal at 298 K.

and 10 MPa, compared with other systems, the diffusion coefficient of CH<sub>4</sub> in coal is the largest when the number of adsorbed H<sub>2</sub>S in coal macromolecule is 0. And as the number of fixed adsorbed H<sub>2</sub>S in the system is larger, the diffusion coefficient of CH<sub>4</sub> in coal molecule is smaller. If there exists H<sub>2</sub>S in the coal seam, the less content of H<sub>2</sub>S is, corresponding to the better diffusion effect of CH<sub>4</sub>.

Because H<sub>2</sub>S molecules and CH<sub>4</sub> molecules exist in the coal seam at the same time, with the gradual increase of the adsorption amount of H<sub>2</sub>S in the coal body, the adsorption amount of CH<sub>4</sub> decreases gradually, and it is not easy to form a large concentration gradient, which increases the diffusion and transport resistance of CH<sub>4</sub> molecules in the coal body, and results in a gradual decrease of the diffusion coefficient and a slowdown of the diffusion rate of CH<sub>4</sub> in the coal body. Since the diffusion movement of CH<sub>4</sub> in the coal seam includes the small-amplitude vibration movement of CH<sub>4</sub> in the pores of the coal body and the jumping movement of CH<sub>4</sub> from one pore space to another due to the relative movement of CH<sub>4</sub> molecules and coal molecules, the pore space of the coal body provides the main place for the diffusion of CH<sub>4</sub> in the coal body, and when H<sub>2</sub>S and CH<sub>4</sub> exist at the same time in the coal seam, due to the competitive adsorption, H<sub>2</sub>S is in an advantageous position compared with CH<sub>4</sub> in the coal body, and H<sub>2</sub>S will preferentially seize the effective adsorption sites in the coal body, occupying a certain amount of the coal body pore space and surface, therefore, the more the adsorption of H<sub>2</sub>S, the more the diffusion sites in the coal body of CH<sub>4</sub> are occupied by H<sub>2</sub>S, and therefore the diffusion of CH<sub>4</sub> in the coal body will be better when the content of H<sub>2</sub>S is less.

## 4. Effect of H<sub>2</sub>S on CO<sub>2</sub> displacement of CH<sub>4</sub> in coal

### 4.1. Ternary gas competitive adsorption

Katayama (Katayama, 1995) was found that N<sub>2</sub> displacement of CH<sub>4</sub> due to partial pressure effect, and the mechanism of CO<sub>2</sub> displacement of CH<sub>4</sub> is due to the difference of adsorption energy between the two. In order to investigate the effect of H<sub>2</sub>S on CO<sub>2</sub> displacement of CH<sub>4</sub> in coal, firstly, we analyse and calculate the magnitude of adsorption energy of LH coal macromolecules on H<sub>2</sub>S, CH<sub>4</sub>, and CO<sub>2</sub>. The isothermal adsorption curves of H<sub>2</sub>S, CH<sub>4</sub> and CO<sub>2</sub> in the pressure range of 0–10 MPa and temperature of 298 K were calculated by using Sorption module, as shown in Fig. 9 below. The calculation results show that with the increase of gas pressure, the adsorption amounts of the three gases in LH coal molecules all show a trend of rapid increase followed by a slow and small increase, and the three isothermal adsorption curves were fitted by Langmuir to obtain the Langmuir volume constant *a* and the



**Table 5**  
Langmuir parameters of each adsorbent in LH coal at 298 K.

| Adsorbate        | $a/(\text{mmol}\cdot\text{g}^{-1})$ | $b/\text{MPa}$ | $R^2$ |
|------------------|-------------------------------------|----------------|-------|
| CH <sub>4</sub>  | 0.908                               | 0.657          | 0.99  |
| H <sub>2</sub> S | 1.790                               | 0.267          | 0.99  |
| CO <sub>2</sub>  | 1.461                               | 0.427          | 0.99  |

Langmuir pressure constant  $b$  in the Langmuir adsorption constants, and the results of the parameters are shown in Table 5.

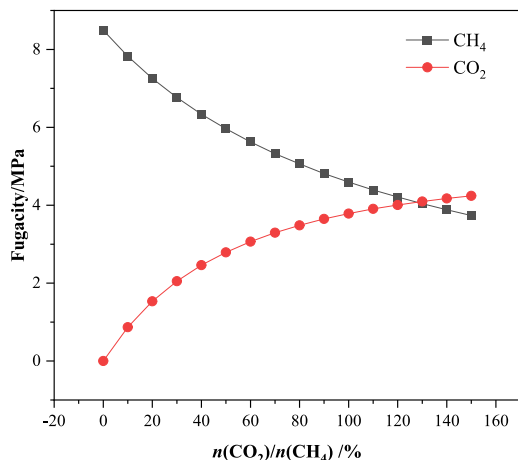
The adsorption of the three gases by coal macromolecules belongs to physical adsorption, the adsorbent molecules are adsorbed on the surface of coal matrix by van der Waals' force, and the different van der Waals' force determines the difference of the adsorption capacity of coal for the three gases. From Fig. 8 and Table 5, it can be found that the saturation adsorption of H<sub>2</sub>S by LH coal macromolecules is the largest under the same temperature and pressure conditions, and its adsorption capacity is in the following order: H<sub>2</sub>S > CO<sub>2</sub> > CH<sub>4</sub>, and the adsorption capacity of LH coal molecules for the three gases in the range of 0–10 MPa increases with the increase of pressure.

According to the previous research, the adsorption capacity of coal for gases is related to the boiling point of adsorbent at 1 atmospheric

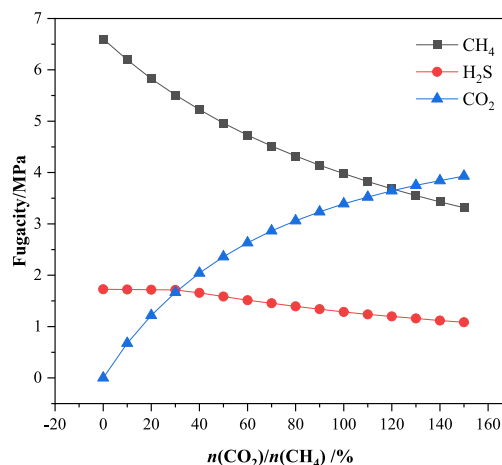
pressure, the higher the boiling point is, the higher the force between the adsorbent and the surface of coal, and the easier it is to be adsorbed in the coal, and the size of the boiling point of three kinds of gases under the condition of atmospheric pressure in the order of H<sub>2</sub>S > CO<sub>2</sub> > CH<sub>4</sub>, and the analysis from the perspective of the boiling point of adsorbent is in accordance with the conclusion obtained from simulation calculations. In addition, the van der Waals force between non-polar molecules and coal surface is smaller than that between polar molecules, H<sub>2</sub>S belongs to polar molecules, and CH<sub>4</sub> and CO<sub>2</sub> belong to non-polar molecules, so the van der Waals force between H<sub>2</sub>S and coal surface is larger, and it is easier to solidify and adsorb. It is known that the kinetic diameter of CO<sub>2</sub> is 0.33 nm, and the kinetic diameter of CH<sub>4</sub> is 0.38 nm, so CO<sub>2</sub> is easier to be adsorbed in coal than CH<sub>4</sub>. In conclusion, from the viewpoint of molecular polarity and molecular diameter, the adsorption capacity of H<sub>2</sub>S > CO<sub>2</sub> > CH<sub>4</sub>, which is in line with the conclusions obtained from the simulation calculations.

#### 4.2. Influence of H<sub>2</sub>S on CO<sub>2</sub> displacement of CH<sub>4</sub>

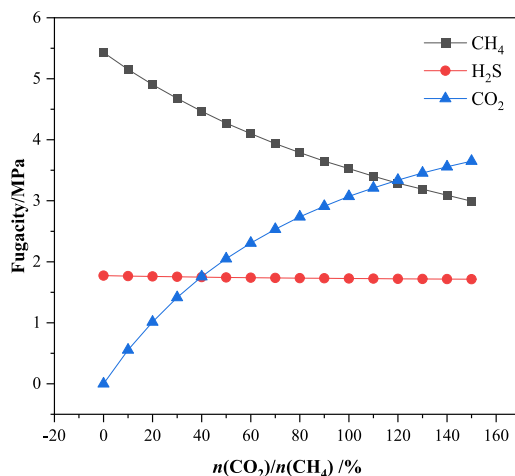
When exploring the effect of H<sub>2</sub>S on CO<sub>2</sub> displacement of CH<sub>4</sub>, considering the actual coal reservoir pressure and for the temperature, the total gas source pressure is taken as 10 MPa, and the temperature is



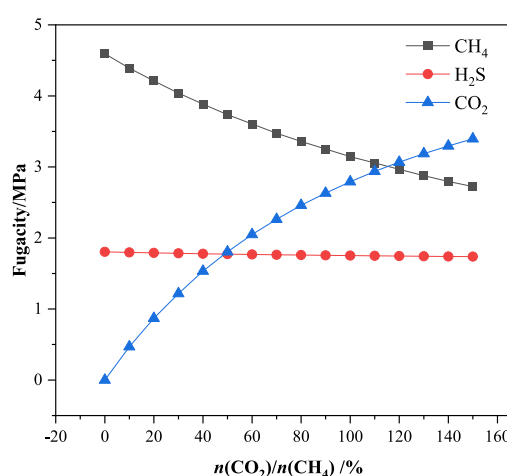
(a)  $n(\text{H}_2\text{S})/n(\text{CH}_4)=0$



(b)  $n(\text{H}_2\text{S})/n(\text{CH}_4)=1/3$



(c)  $n(\text{H}_2\text{S})/n(\text{CH}_4)=2/3$



(d)  $n(\text{H}_2\text{S})/n(\text{CH}_4)=1$

Fig. 10. Corresponding fugacity of each component for different mixture ratios.

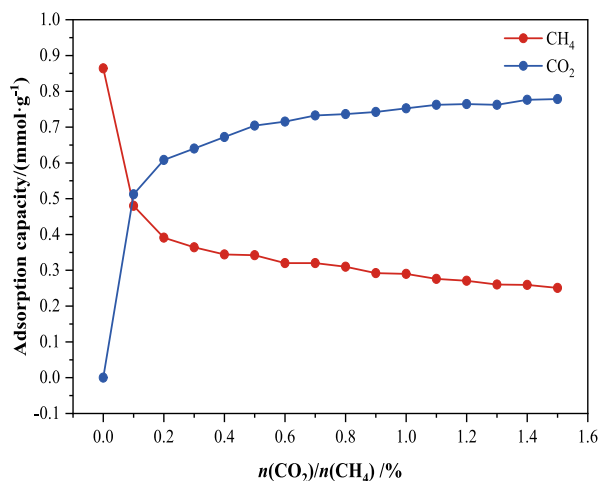
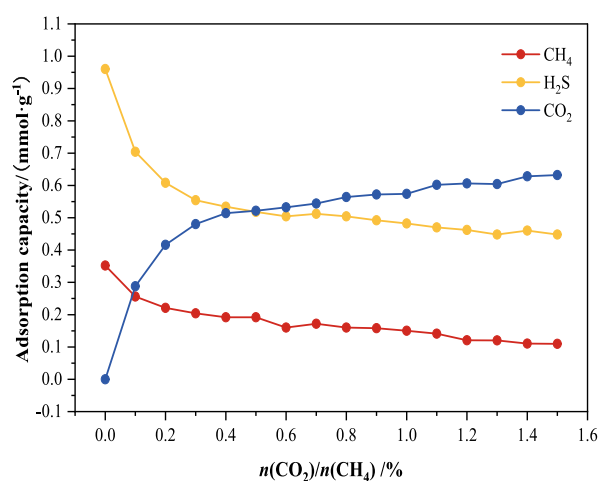
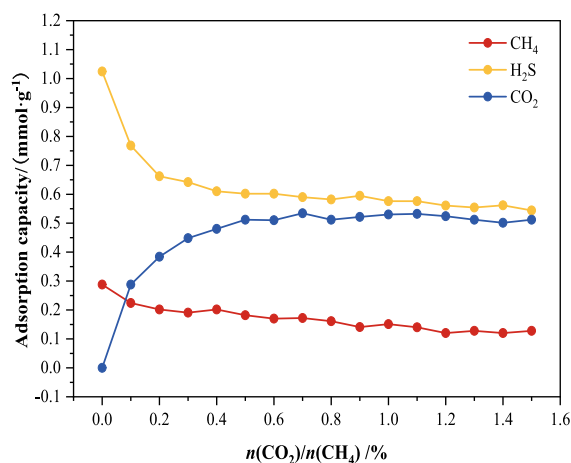
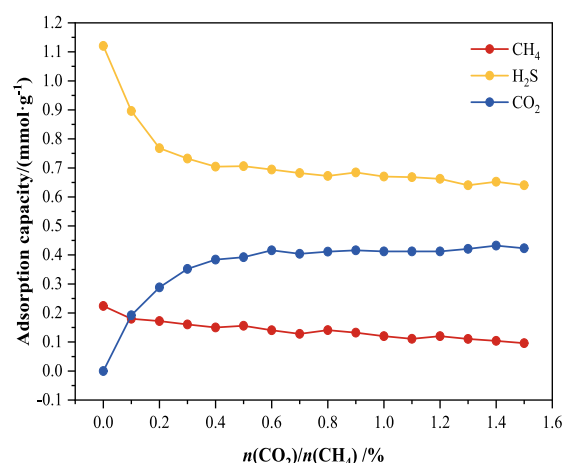
(a)  $n(\text{H}_2\text{S})/n(\text{CH}_4)=0$ (b)  $n(\text{H}_2\text{S})/n(\text{CH}_4)=1/3$ (c)  $n(\text{H}_2\text{S})/n(\text{CH}_4)=2/3$ (d)  $n(\text{H}_2\text{S})/n(\text{CH}_4)=1$ 

Fig. 11. Adsorption curves of components in LH coal under different mixture conditions.

set to 298.15 K. It can be obtained from Eq. (5), the saturated adsorption amount of LH coal macromolecule  $\text{CH}_4$  is 0.83 mmol/g. With the help of Matlab software, the required pressure ( $p$ ) for each component of  $\text{CH}_4$ ,  $\text{H}_2\text{S}$ ,  $\text{CO}_2$  under the condition of mixture ratio is converted into the required fugacity value ( $f$ ) for MS-sorption module by using P-R equation of state, and the corresponding fugacity values of each component in different mixture ratios are shown in Fig. 10.

Using the Sorption-Fixed pressure task, the temperature was set to 298 K, and the fugacity values of each component of the ternary mixture were set according to the above ratio, which resulted in the isothermal adsorption curves corresponding to the three components in the mixture when the molar fractions of  $\text{H}_2\text{S}$  accounted for  $\text{CH}_4$  were 0, 1/3, 2/3, and 1, respectively, as shown in Fig. 11.

From the data in Fig. 10, it can be obtained that the larger the proportion of  $\text{H}_2\text{S}$  in the adsorbent, the less the pressure that  $\text{CO}_2$  shares in the case of the total pressure remains constant, and from the perspective of the gas partial pressure this will be unfavourable to the effect of  $\text{CO}_2$  on the displacement of  $\text{CH}_4$  in the coal seam. Analysing Fig. 11, it can be obtained that the number of  $\text{H}_2\text{S}$  adsorbed in LH coal in the four group

system gradually decreases due to the partial pressure, the number of  $\text{CO}_2$  adsorbed in LH coal increases with the increase of the proportion of  $\text{CO}_2$  in the mixed gas, and the larger the proportion of  $\text{H}_2\text{S}$  in the mixed gas, the smaller the increase in the adsorption amount of  $\text{CO}_2$ . When  $n(\text{H}_2\text{S})/n(\text{CH}_4) = 1/3$  in the mixture system, the adsorption amount of  $\text{CO}_2$  in LH coal macromolecules gradually increased, and the adsorption amount of  $\text{H}_2\text{S}$  appeared to be greatly reduced, and when  $n(\text{CO}_2)/n(\text{CH}_4) > 0.5$ , the adsorption amount of  $\text{CO}_2$  in LH coal macromolecules exceeded that of  $\text{H}_2\text{S}$  and  $\text{CH}_4$ . The main reason for this result is that the adsorption capacity of adsorbed gas in coal increases with the increase of gas pressure due to the obvious increase of  $\text{CO}_2$  pressure under the partial pressure of mixed gas. When  $n(\text{H}_2\text{S})/n(\text{CH}_4) > 1/3$  in the gas mixture system, the adsorption amount of  $\text{H}_2\text{S}$  in LH coal is always larger than the adsorption amount of  $\text{CO}_2$  and  $\text{CH}_4$  in the investigated range, because in addition to the effect of partial pressure, due to the adsorption capacity of LH coal molecules on  $\text{H}_2\text{S}$  is stronger than  $\text{CO}_2$  and  $\text{CH}_4$ , and the competition adsorption plays a more obvious role in this stage, so the adsorption amount of  $\text{H}_2\text{S}$  is more than that of  $\text{CO}_2$  and  $\text{CH}_4$ . Comparing the data in Fig. 11 (a) and (b) (c) (d), it can be seen that when

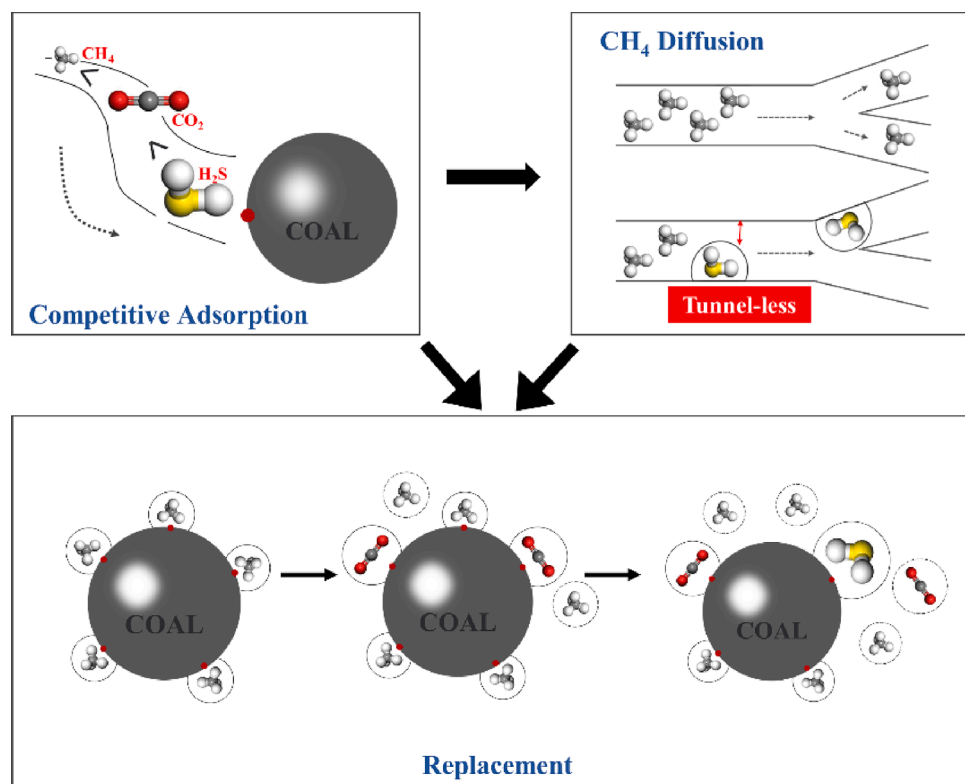


Fig. 12. Schematic diagram of the effect of H<sub>2</sub>S on CH<sub>4</sub> adsorption, diffusion and displacement.

the adsorbent system does not contain H<sub>2</sub>S, with the increase of the mole fraction of CH<sub>4</sub> accounted for by CO<sub>2</sub> in the mixture from 0 % to 150 %, the decrease in the number of CH<sub>4</sub> adsorbed molecules in LH coal is significantly stronger than that when there is a gas of H<sub>2</sub>S in the mixture and the greater the proportion of H<sub>2</sub>S in the system, the smaller the decrease in the adsorbed amount of CH<sub>4</sub>. This indicates that under the influence of H<sub>2</sub>S, LH coal molecules preferentially adsorb H<sub>2</sub>S molecules, and compared with CO<sub>2</sub> molecules, H<sub>2</sub>S preferentially occupies the adsorption sites, which affects the displacement effect of CO<sub>2</sub> on CH<sub>4</sub> in LH coal molecules.

In summary, combining the results of single-component and CH<sub>4</sub>/CO<sub>2</sub> two-component adsorption, as shown in Fig. 12, due to the difference in the adsorption energy of coal molecules on H<sub>2</sub>S, CO<sub>2</sub> and CH<sub>4</sub>, the adsorption of CH<sub>4</sub> and CO<sub>2</sub> in the coal will be inhibited when H<sub>2</sub>S is present in the system. Due to competitive adsorption, H<sub>2</sub>S preferentially adsorbs on the surface and pores of coal, hindering the diffusion behavior of CH<sub>4</sub> in the coal, and the slow diffusion of CH<sub>4</sub> in the coal will directly restrict the extraction efficiency of coal seam gas, and H<sub>2</sub>S in the coal seam to preempt the adsorption site of CO<sub>2</sub> in coal, resulting in a reduction in the rate of resolution of CH<sub>4</sub> when the CO<sub>2</sub> displacement of CH<sub>4</sub>. It can be seen that if CO<sub>2</sub> is used to displace CH<sub>4</sub> in coal mines containing H<sub>2</sub>S, it is recommended to increase the volume fraction of CO<sub>2</sub> in the displacement gas appropriately or to complete the treatment of H<sub>2</sub>S in the coal seam before the displacement of coal seam gas.

## 5. Conclusions

This paper investigates the effect of H<sub>2</sub>S on the diffusion and displacement characteristics of CH<sub>4</sub> in coal, focusing on the adsorption and diffusion process of methane in coal in the presence of H<sub>2</sub>S, constructs a molecular model of coal through physical structure characterization experiments, and calculates the simulation of the mono-, bi-, and ternary adsorption of H<sub>2</sub>S, CH<sub>4</sub>, and CO<sub>2</sub> in coal using molecular simulation, and the main conclusions were drawn as follows:

(1) Through industrial analysis, elemental analysis, <sup>13</sup>C NMR, FTIR

and XPS coal chemical structure physical testing experiments, the molecular planar model of LH coal was analysed and obtained, and its molecular formula is C<sub>212</sub>H<sub>156</sub>O<sub>9</sub>N<sub>2</sub>S<sub>3</sub>. The LH 3D coal macromolecular structure model constructed by MS is reasonable after density test.

(2) H<sub>2</sub>S in the system will preferentially seize the adsorption sites of the coal body and inhibit the adsorption of CH<sub>4</sub> molecules by the coal body. Analysing and calculating the MSD curves of the saturated adsorption model of CH<sub>4</sub> in coal under different conditions, it can be seen that the lower the content of H<sub>2</sub>S is, the better the corresponding CH<sub>4</sub> diffusion effect, the presence of H<sub>2</sub>S in the system will inhibit the diffusion of CH<sub>4</sub> in coal.

(3) Under the same temperature and pressure, the adsorption capacity of coal macromolecules on CH<sub>4</sub>, H<sub>2</sub>S and CO<sub>2</sub> is in the following order: H<sub>2</sub>S > CO<sub>2</sub> > CH<sub>4</sub>, which is consistent with the results of the size of the boiling point of the adsorbent, the polarity of the molecule and the size of the molecular dynamics diameter.

(4) Due to the difference in the adsorption energy of coal macromolecules on H<sub>2</sub>S, CO<sub>2</sub> and CH<sub>4</sub>, the adsorption amount of CO<sub>2</sub> in coal is obviously reduced when H<sub>2</sub>S exists in the system, and the reduction of adsorption capacity of CH<sub>4</sub> is significantly reduced compared with that when only CO<sub>2</sub>/CH<sub>4</sub> two-component gas is present in the system, that is, H<sub>2</sub>S has a significant inhibition effect on CO<sub>2</sub> displacement of CH<sub>4</sub> in coal.

Further analysis and research on the factors affecting the diffusion and displacement characteristics of CH<sub>4</sub> in coal will help to improve the mechanism of coalbed methane storage and transport, and will be of great engineering significance for the efficient extraction of gas from H<sub>2</sub>S-containing coal mines.

## CRediT authorship contribution statement

**Jinyu Li:** Conceptualization, Formal analysis, Funding acquisition, Writing – original draft, Writing – review & editing. **He Ji:** Conceptualization. **Zunguo Zhang:** Software. **Gang Bai:** Formal analysis. **Hongbao Zhao:** Formal analysis. **Xihua Zhou:** Methodology. **Yueran**

Wang: Formal analysis. Yixin Li: Data curation.

### Declaration of competing interest

The authors declare that they have no known competing financial interests or personal relationships that could have appeared to influence the work reported in this paper.

### Acknowledgments

This work was financially supported by the Scientific Research Funding project of National Natural Science Foundation of China (52304086, 52274204), Young Elite Scientists Sponsorship Program by CAST (2022QNRC001) and LiaoNing Revitalization Talents Program (XLYC2008021).

### References

- Fan, C.J., Xu, L.J., Elsworth, D., Luo, M.K., Liu, T., Li, S., Zhou, L.J., Su, W.W., 2023. Spatial-temporal evolution and countermeasures for coal and gas outbursts represented as a dynamic system. *Rock Mech. Rock Eng.* 56, 6855–6877.
- He, Y., Fu, X.M., Lu, L., 2016. Differences of H<sub>2</sub>S, CH<sub>4</sub> and N<sub>2</sub> adsorption ability on coal. *China Sciencepaper* 11 (15), 1775–1777+1796.
- Jiang, J.Y., Peng, H.Z., Cheng, Y.P., Wang, L., Wang, C.H., Ju, S., 2022. Effect of moisture on time-varying diffusion properties of methane in low-rank coal. *Transport Porous Med.* 146 (3), 617–638.
- Jing, G.X., Mu, L.L., 2023. Study on statistical analysis and emergency management of coal mine gas explosion accident. *J. Saf. Environ.* 23 (10), 3657–3665.
- Yukuo Katayama, 1995. Study of Coalbed Methane in Japan. *Proceedings of United Nations international conference on coalbed methane development and utilization.*
- Liang, Y.P., Zheng, M.H., Li, Q.G., Mao, S.R., Li, X.Y., Li, J.B., Zhou, J.J., 2023. A review on prediction and early warning methods of coal and gas outburst. *J. China Coal Soc.* 48 (8), 2976–2994.
- Liu, H., 2020. Hydrogen Sulfide Adsorption Characteristics and Treatment of Sulfur-bearing Coal Seam. Xi'an University of Science and Technology (Xi'an).
- Meng, Y., Li, Z.P., 2016. Experimental study on diffusion property of methane gas in coal and its influencing factors. *Fuel* 185 (1), 219–228.
- Meng, Z.P., Zhang, G.Y., Li, G.Q., Liu, J.R., 2019. Analysis of diffusion properties of methane in low rank coal. *Coal Geol. Explor.* 47 (2), 84–89.
- Rubright, S.L.M., Pearce, L.L., Peterson, J., 2017. Environmental toxicology of hydrogen sulfide. *Nitric Oxide Biol. Ch.* 71, 1–13.
- Sun, Z.X., Min, C., Zhang, W.L., Zhang, Y.P., Yu, X.F., Cui, B., 2022. Molecular simulation study on the effect of CO<sub>2</sub>/N<sub>2</sub> binary gas on methane adsorption in coal. *Coal Geol. Explor* 50 (3), 127–136.
- Tan, B., Shao, Z.Z., Wei, H.Y., Yang, G.Y., Zhu, X.M., Xu, B., Zhang, F.C., 2020. Status of research on hydrogen sulphide gas in Chinese mines. *Environ. Sci. Pollut. r.* 27 (3), 2502–2521.
- Tang, J.P., Qiu, Y.M., Ma, Y., 2021. Molecular dynamics analysis of influencing factors of CH<sub>4</sub> diffusion in coal. *Coal Sci. Technol.* 49 (2), 85–92.
- Wang, J.R., Ding, C., Gao, D.M., Liu, H.P., 2020. Research on adsorption characteristics of H<sub>2</sub>S, CH<sub>4</sub>, N<sub>2</sub> in coal based on Monte Carlo method. *Sci. Rep. UK* 10, 21882.
- Xu, L.J., Fan, C.J., Luo, M.K., Li, S., Han, J., Fu, X., Xiao, B., 2023. Elimination mechanism of coal and gas outburst based on geo-dynamic system with stress–damage–seepage interactions. *IJCST* 10, 74.
- Xue, J.Z., Fu, X.H., Wu, J.H., Ding, Y.M., 2017. Adsorption characteristics of H<sub>2</sub>S in coal mine gas and their effect on H<sub>2</sub>S control in coal mines. *Geol. Explor.* 53 (3), 609–614.
- Yang, S.B., Wang, H.C., Fu, X.H., Tian, J.J., Zhao, F.Y., Wang, Z., Sun, P.C., Cao, Y.Z., 2022. Hydrogen sulfide occurrence states in China's coal seams. *Energ. Explor. Exploit.* 40 (1), 17–37.
- Zhang, Q.G., Li, Q.S., Fan, X.Y., Liu, C., Ge, Z.L., Jiang, Z.G., Peng, X.L., Li, X.C., Zhu, S. Y., Zhao, S.L., Zhao, P.F., Chen, Y.F., 2022. Current situation and development trend of theories and technologies for coal and CBM co-mining in China. *Nat. Gas Ind.* 42 (6), 130–145.
- Zhang, C., Wang, X.L., Liu, H., Liu, C., Zeng, X., 2020. Development and application of modified lye for treating hydrogen sulphide in coal mine. *Fuel*, 269(1),117233.1-117233.9.
- Zhao, Y.L., Feng, Y.H., Zhang, X.X., 2016. Molecular simulation of CO<sub>2</sub>/CH<sub>4</sub> self- and transport diffusion coefficients in coal. *Fuel* 165 (1), 19–27.
- Zhao, J.L., Tang, D.Z., Xu, H., Li, S., Tao, S., Zhai, Y.Y., Liang, W., Lin, W.J., Huo, X.S., 2016. Measurement of methane diffusion coefficient and analysis of its influencing factors in coal matrix. *Coal Sci. Technol.* 44 (10), 77–82+145.
- Zhou, R.X., 2021. Study on Gas Adsorption Characteristics of Coal Seams Containing Hydrogen Sulfide Based on Molecular Simulation. Chongqing University (Chongqing).